ELSEVIER

Polymer 43 (2002) 3699–3705

polymer

www.elsevier.com/locate/polymer

Structure–property relationships in cross-linked polyester–clay nanocomposites

R.K. Bharadwaj[a,*], A.R. Mehrabi[a], C. Hamilton[a], C. Trujillo[a], M. Murga[a], R. Fan[a], A. Chavira[a], A.K. Thompson[b]

[a]*Avery Research Center, 2900 Bradley Street, Pasadena, CA 91107, USA*
[b]*Center for Electron Microscopy and Microanalysis, University of Southern California, Los Angeles, CA 90089, USA*

Received 3 December 2001; received in revised form 22 February 2002; accepted 26 February 2002

Abstract

Crosslinked polyester–clay nanocomposites were prepared by dispersing organically modified montmorillonite in prepromoted polyester resin and subsequently crosslinked using methyl ethyl ketone peroxide catalyst at several different clay concentrations (1.0, 2.5, 5.0, and 10.0 wt%). X-ray diffraction studies revealed the formation of a nanocomposite in all cases with the disappearance of the peak corresponding to the basal spacing of the pure clay. Transmission electron microscopy was used to study the morphology at different length scales and showed the nanocomposite to be comprised of a random dispersion of intercalated/exfoliated aggregates throughout the matrix. Thermal degradation of the nanocomposites was found to be slightly but progressively hastened compared to the pure crosslinked polymer, loss and storage modulus were monotonically shifted toward higher frequency values, and the tensile modulus was found to decrease with increasing clay content. These unexpected results were rationalized based on the decrease in the degree of crosslinking of the polyester resin in the nanocomposite, in the presence of clay. In particular, the nanocomposite containing 2.5 wt% clay consistently demonstrated a drop in properties far greater than that observed at other clay concentrations, and was attributed to the greater degree of exfoliation seen in this case which presumably leads to a greater decrease in the degree of crosslinking. Oxygen permeability rates in the polyester nanocomposites decreased with increasing clay content, as expected, and was satisfactorily reproduced using a tortuosity based model.

Keywords: Polyester–clay nanocomposites; X-ray diffraction; Structure–property relationships

1. Introduction

There is now a considerable body of literature since the seminal work by the Toyota research group [1–3] demonstrating that nanoscopic dispersion of platelet-like structures such as clays (aluminosilicates) in a polymeric matrix results in remarkable property enhancements. For example, dramatic improvements in the stiffness and strength [1–6], increased dimensional stability [7,8], improved flame retardancy [9,10], improved solvent and UV resistance [11,12], and reduction in permeability to gases [13–17] have been reported in a wide range of polymers. Most notably, the property improvements resulting from the formation of a nanocomposite occur at extremely low concentrations of the aluminosilicate (1–5 vol%) compared to conventional phase-separated composites of a filler material in a polymer (20–30 vol%). The extremely large surface area available for interactions with a polymeric matrix coupled with high aspect ratio (between 30 and 2000) are largely responsible for the observed enhancements. Clays or layered aluminosilicates are crystalline materials consisting of 1 nm thick layers (or sheets) which are made up of an octahedral sheet of alumina fused to two tetrahedral sheets of silica. These layers are essentially polygonal two-dimensional sheets, possessing a thickness of ~1 nm and ranging between 30 and 2000 nm in diameter. Frequently, isomorphic substitutions in these sheets lead to a net negative charge necessitating the presence of cationic counter-ions in the inter-sheet region or gallery spacing. The counter-ions are frequently exchanged with organic alkyl ammonium modifiers that lead to more favorable interactions with a polymer.

Morphological descriptors such as intercalation and exfoliation are commonly used to describe the state of aggregation of the individual sheets of clay in the polymer. The former refers to the state where the gallery regions between the aluminosilicate sheets are swollen by polymer

* Corresponding author. Tel.: +1-626-398-2538; fax: +1-626-398-2553.
E-mail address: rishikesh_bharadwaj@averydennison.com (R.K. Bharadwaj).

0032-3861/02/$ - see front matter
PII: S0032-3861(02)00187-8

chains while retaining the regular stacking arrangement. The latter generally represents the situation where the sheets are completely delaminated and dispersed in the matrix. It is important to note that a distinct morphological hierarchy is extant in polymer–clay nanocomposites that is difficult to capture with the aid of just two morphological descriptors. Three routes, in situ polymerization [2,11,18], solvent casting [19,20] and melt compounding [6,21] techniques may be used to prepare polymer nanocomposites. All the three methods involve the precise matching of interactions between the polymer/monomer and the aluminosilicate, which generally represents the limiting step in nanocomposite formation.

Kornmann et al. [22] reported dispersions of montmorillonite clay in unsaturated polyester resin that lead to cured composites that displayed partial delamination of the aluminosilicate. They found that the fracture toughness doubled by dispersing merely 1.5 vol% of aluminosilicate with concomitant increases in other mechanical properties. Suh et al. [23] demonstrated that the resulting properties of polyester–clay nanocomposites were greatly dependent on the preparation procedure with regard to the order of mixing of the clay, polyester resin and promoter (styrene monomer), as well as, the curing conditions. In this work, we report the preparation and characterization of polyester–clay nanocomposites crosslinked at room temperature with an aim to establish the structure–property relationships extant in these systems. In particular, establishing the morphological hierarchy extant at different length scales (several microns versus several hundred nanometers), and its connection to the macroscopically observed properties form the theme of this work.

2. Experimental details

2.1. Nanocomposite preparation

Clear-Lite®, a pre-promoted, water-clear, casting polyester resin was obtained from TAP Plastics. Cloisite® 30B, a natural montmorillonite modified with methyl tallow bis-2-hydroxyethyl quaternary ammonium chloride was mixed with the low viscosity polyester resin to prepare the nanocomposites was obtained from Southern Clay Products. This particular organically modified clay was chosen due to the presence of the polar hydroxyl group that presumably provides a good wetting surface for the unsaturated polyester. Several different clay concentrations in the crosslinked polyester resin were investigated (1, 2.5, 5, and 10 wt%). These wt% concentrations correspond to 0.5, 1.4, 2.8 and 5.8 vol%, converted using a density of 1.10 g cm^{-3} for the cured polyester resin and 1.98 g cm^{-3} for the Cloisite® 30B nanoclay. We note that the concentrations reported are total concentrations, which include the contribution from the organic modifier. An appropriate amount of the organically modified clay was added to the resin and mechanically stirred followed by sonication for 1 h, which resulted in well-dispersed, stable suspensions of the clay in the polyester resin. Crosslinking was initiated by adding ~1.5 vol% of MEKP catalyst to the resin–clay mixture at room temperature as recommended by the manufacturer. The crosslinking reaction was noticeably slower at the higher clay concentrations (>2.5 wt%). Samples were allowed to cure for at least 24 h at room temperature before initiating analysis. Fresh batches of polyester–clay mixtures were prepared using the above method for each characterization experiment.

2.2. Characterization

Wide-angle X-ray diffraction measurements were performed on the crosslinked polyester–clay samples with a Rigaku RV20 diffractometer using Cu Kα radiation in the 2θ range 2–10°. Transmission electron microscopy (TEM) was performed on a JEOL 100CXII microscope on ~100 nm thick sections, microtomed from samples containing 2.5 and 10.0 wt% clay. Thermogravimetric analysis (TGA) was performed using a TA instruments TGA2950 with samples being heated to 650 °C in N_2 and up to 750 °C in air at a rate of 10 °C min^{-1}. Tensile test was performed on an Instron 5542 at a rate of 5 in. min^{-1} at 50% relative humidity and 23 °C. Tensile test samples were cast in molds that were 22 mm in length and 5 mm wide and ~1 mm thick. Samples for measuring the O_2 permeability rates were prepared by spreading a small quantity of the resin containing MEKP catalyst between two 2 mil thick PET films and calendered together to produce a uniform multi-layer construction and subsequently cured. The O_2 transmission rate through the films was measured on a MOCON OX-TRAN 2/20 unit at 40 °C and 90% relative humidity. Rheological data of the polyester–clay nanocomposites was generated in the frequency range of 0.1–100 rad s^{-1} and at temperatures between 0 and 90 °C in 10 °C intervals using a RSAII rheometer. Master curves were made by horizontally shifting the storage modulus (G') versus radial frequency curves at different temperatures using a reference temperature of 21 °C. Samples for light transmittance measurement were prepared by placing a drop of the resin–clay–catalyst mixture on a clean glass plate and placing a glass cover slide and gently applying pressure to spread the resin uniformly and crosslinked subsequently. A Biotek Instruments μQuant spectrophotometer was used to measure the % transmission using a wavelength of 400 nm.

3. Results and discussion

3.1. Structure and morphology

It is useful to start by establishing the morphological state of the crosslinked polyester–clay nanocomposites. This has been accomplished by using X-ray diffraction and TEM. The X-ray scattering intensities for the organically modified

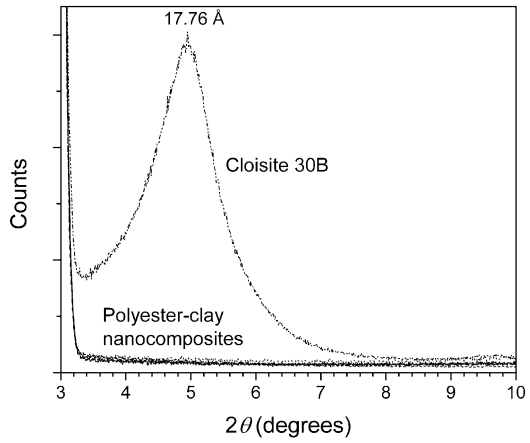

Fig. 1. X-ray scattering profiles for Cloisite® 30B (organically modified montmorillonite clay) and crosslinked polyester nanocomposites containing 1, 2.5, 5 and 10 wt% of Cloisite® 30B clay.

clay, Cloisite® 30B, and the polyester–clay nanocomposites containing different concentrations of clay are shown in Fig. 1. In the scattering curve for the pure clay, a prominent peak corresponding to the basal spacing of Cloisite® 30B organically modified montmorillonite occurs at a *d*-spacing of 17.8 Å. This reflection is absent in the scattering curves for all the polyester–clay nanocomposites, irrespective of clay concentration, confirming the formation of a nanocomposite. The presence of order at higher *d*-spacing (>26 Å or 3.5 ° 2θ) could not be confirmed from the data.

TEM allows the morphological state of the nanocomposite to be delineated more completely. It is instructive to consider the structural hierarchy of clay particles as a prelude to understanding the morphology of the polymer nanocomposite evidenced in the micrographs. Montmorillonite clay consists of a hierarchy of structures, of which the individual aluminosilicate sheets (~1 nm thick) may be considered the basic structural unit. Several sheets stacked face to face with an interlayer charge balancing cation lead to a stack and an agglomeration of these stacks leads to the macroscopically observable micron-sized particles. Therefore, each macroscopic particle of clay is actually comprised of many individual aluminosilicate sheets. Consequently, the formation of a nanocomposite involves the break-up and dispersion of the agglomerated stacks of sheets followed by the swelling of the gallery spacing between the sheets by the polymer/monomer.

The TEM micrographs shown in Figs. 2 (2.5 wt%) and 3 (10.0 wt%) attempt to demonstrate this hierarchy and its preservation in the final nanocomposite by using different magnifications in the imaging. Low magnification micrographs, Figs. 2(a) and 3(a), show the dispersion of micron-sized aggregates of sheets in the matrix. Fewer aggregates are observed in Fig. 2(a) since the concentration of clay is accordingly lower (2.5 wt%) in this case. Increasing the magnification in an area occupied by an aggregate reveals the individual sheets of clay clearly separated by a layer of polymer as shown in Figs. 2(b) and 3(b). It is

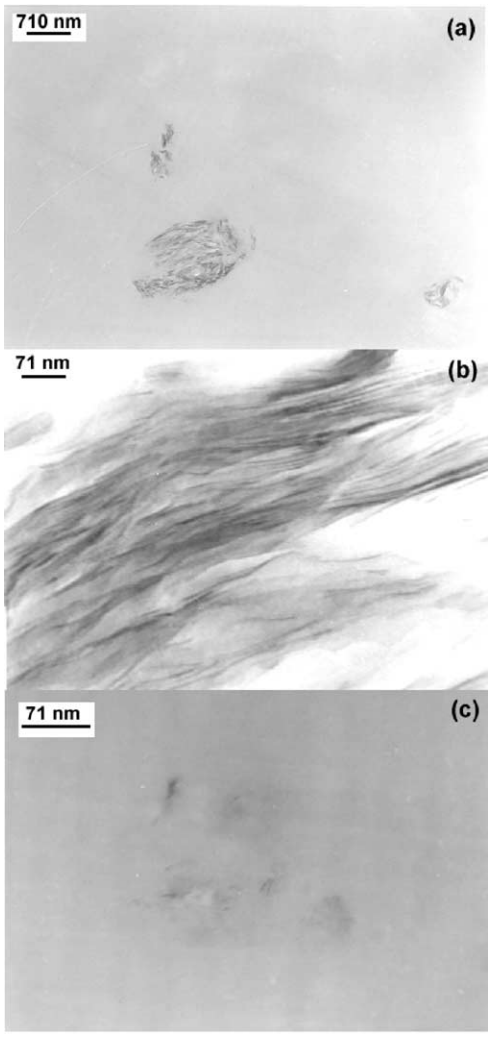

Fig. 2. TEM micrographs of crosslinked polyester nanocomposite containing 2.5 wt% clay showing: (a) microstructure at low magnification and (b) intercalated and exfoliated sheets at high magnification of the aggregate region shown in (a), and (c) fully exfoliated sheets.

evident that the morphology may be considered a mix of intercalated and exfoliated sheets. That is, there are regions where the regular stacking arrangement is maintained with a layer of polymer between the sheets, and also regions where completely delaminated sheets are dispersed individually. In the case of the 2.5 wt% clay containing nanocomposite, regions such as those shown in Fig. 2(c) were detected showing individual dispersion of completely delaminated sheets in the matrix. There appears to be some evidence supporting the formation of an exfoliated morphology at a more global scale in the 2.5 wt% polyester–clay nanocomposite. It is also noted that a high degree of orientational order of the aluminosilicate sheets is present within the stacks of the intercalated and exfoliated aggregates. The evidence shown here in Figs. 2 and 3 clearly demonstrates the need for the microstructure to be investigated at different magnifications to establish the hierarchy. In the interest of clarity, the morphology extant in the nanocomposites

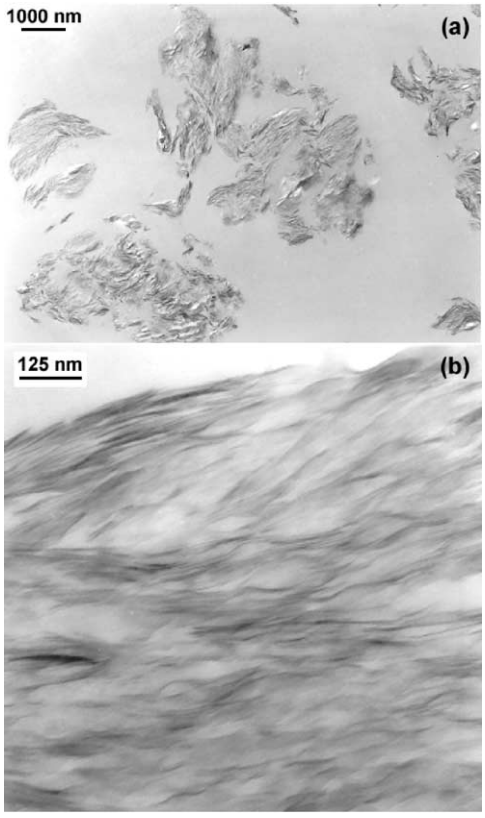

Fig. 3. TEM micrographs of crosslinked polyester nanocomposite containing 10.0 wt% clay at: (a) low and (b) high magnifications. Both intercalated and locally exfoliated regions may be discerned.

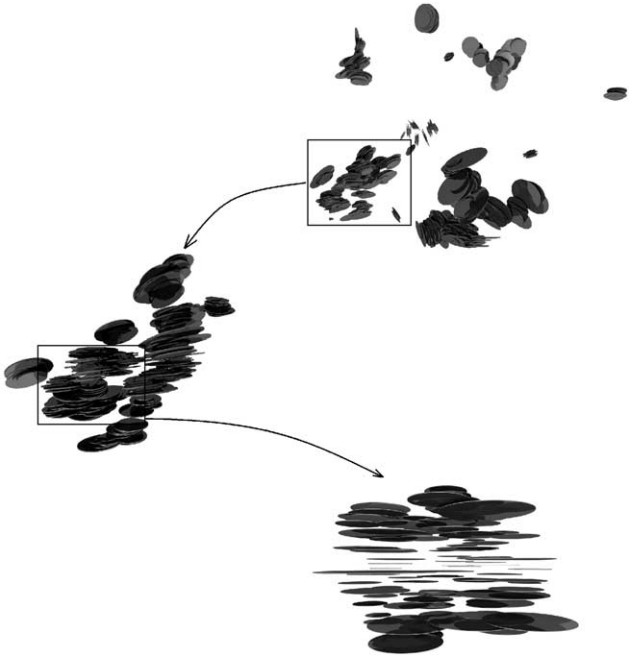

Fig. 4. Illustration of the morphological hierarchy at different length scales extant in the polyester–clay nanocomposites showing the dispersion of intercalated/exfoliated aggregates throughout the matrix and the local orientational ordering of the sheets within the aggregates.

delineating this structural hierarchy has been shown in Fig. 4. This essentially conveys a three-dimensional perspective of the morphology at different length scales. Establishing local versus global morphology and orientational order of the sheets is central to efficient characterization of nanocomposite structures. For example, a situation may be envisaged where the clay sheets are completely delaminated and homogeneously dispersed throughout the matrix, or there may be localized regions of exfoliated sheets dispersed throughout the matrix. These two situations presumably result in nanocomposites that are completely different in terms of properties and determining this difference may hold the key to understanding the macroscopic behavior. This argument points to the clear need for the development of more robust morphology descriptors in nanocomposites that takes into account both the short and long-range order and dispersion of the aluminosilicate sheets. Notwithstanding the issues discussed earlier, it can be concluded that the morphology of the crosslinked polyester–clay nanocomposites can be described as a dispersion of intercalated and exfoliated aggregates in the matrix.

3.2. Thermal analysis

Perhaps the most curious behavior of the crosslinked polyester–clay nanocomposites reported here is manifested in the thermal degradation. One of the most important property enhancements expected upon formation of a polymer nanocomposite is in the retardation of the thermal degradation [20,24]. TGA of the crosslinked polyester nanocomposites displays the exact opposite behavior. The onset of degradation is slightly but progressively hastened upon addition of clay to the nanocomposites as compared to the pure polymer seen in Fig. 5. The pure polymer is completely decomposed at 400 °C. The nanocomposites degrade at a faster rate in the temperature range 25–400 °C compared to the pure polymer and thereafter the situation reverses.

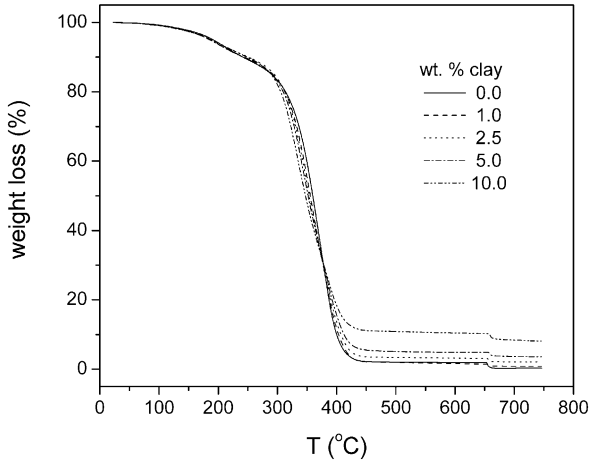

Fig. 5. TGA thermal degradation profiles for the crosslinked polyester–clay nanocomposites at different concentrations of clay. Samples were heated from 23 to 650 °C in nitrogen and 650 to 750 °C in air.

It is not surprising that the nanocomposites show slower degradation above 400 °C since there is only inorganic aluminosilicate left in the system at that stage. The monotonic increase in the rate of degradation in the nanocomposites may be due to the presence of increasing amount of hydroxyl groups in the organic modifier that provides a supply of oxygen.

3.3. Dynamic mechanical analysis and mechanical properties

The rheological properties of the crosslinked polyester–clay nanocomposites are shown in the form of the frequency dependence of the storage (G') and loss (G'') modulus in Fig. 6. The behavior manifested in the G' and G'' is remarkable in many respects. First, the G' and G'' values decrease monotonically with increasing clay concentration whereas, the exact opposite is expected for a nanoscopically reinforced polymer [26]. Second, the G' and G'' curves follow from left to right in Fig. 6 in the order 0.0, 1.0, 5.0, 2.5 and 10.0 wt%. That is, G' and G'' values are lower for 2.5 wt% case compared to the 5.0 wt% case.

The dependence of the tensile modulus on the clay concentration shown in Fig. 7, bears out the earlier observations. First, the tensile modulus is seen to decrease with increasing clay content, and second, the drop in the value

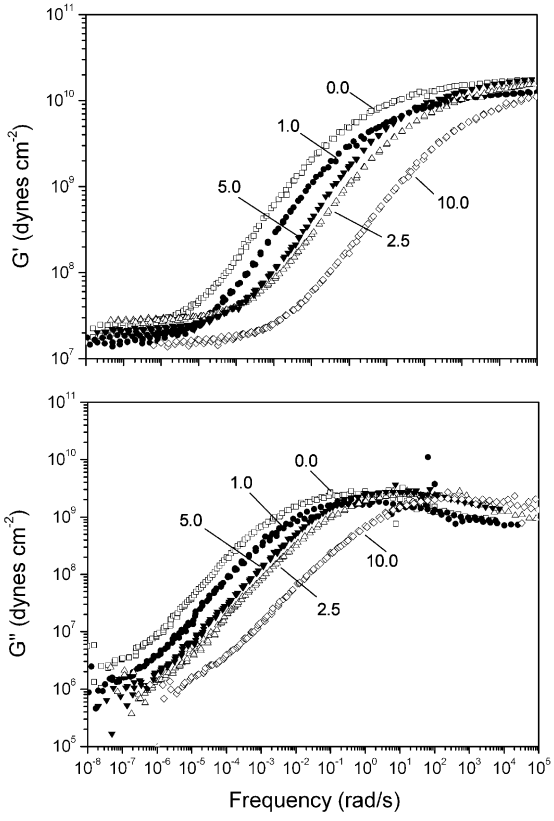

Fig. 6. Storage (G') and loss (G'') modulus as a function of radial frequency for the crosslinked polyester–clay nanocomposites at different clay concentrations.

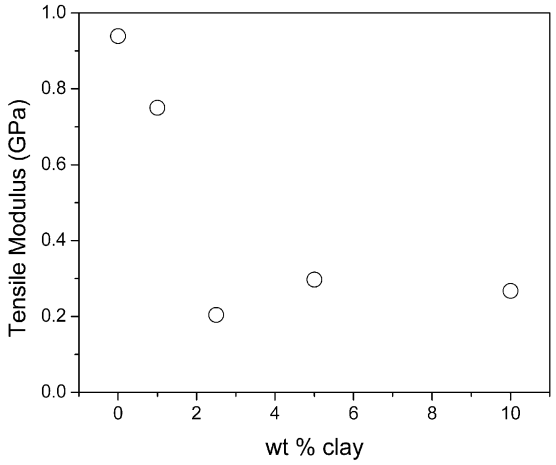

Fig. 7. Tensile modulus versus clay concentration for the crosslinked polyester nanocomposites as determined at 23 °C and 50% relative humidity.

for the 2.5 wt% nanocomposite is greater than expected. A combination of the morphology and the extent of crosslinking in the polyester–clay nanocomposites can be used to understand this phenomenon. It is proposed that the intercalation and exfoliation of the clay in the polyester resin serves to effectively decrease the number of crosslinks from a topological perspective. The overall decrease in the G', G'', and tensile modulus of the polymer nanocomposites with increasing clay content lend credence to the hypothesis that the degree of crosslinking is indeed reduced. The origin of the greater drop in properties of the 2.5 wt% nanocomposite may be traced to the morphology shown in Fig. 2(c), where it was observed that the sample showed exfoliation on a more global scale compared to the 10 wt% sample. In terms of the explanation put forth, the crosslink density is inversely proportional to the degree of exfoliation and macroscopic dispersion. Permeability studies discussed in Section 3.4 also bear out these observations, as well as, lending further support to the explanation put forth.

3.4. O_2 permeability

The gas barrier properties have been shown to improve dramatically upon exfoliation of clay platelets in a number of polymeric matrices [13–17]. The mechanism for the improvement is attributed to the increase in the tortuosity of the diffusive path for a penetrant molecule. Indeed, a simple tortuosity based model [27,28] has been found to reproduce experimental trends satisfactorily [13–16]. This observation is surprising, essentially implying that the nanoscale interactions between the polymeric matrix and the clay sheets do not change the thermodynamic solubility of the penetrant significantly. The permeability of the nanocomposite (P_s) is related to the permeability of the pure polymer (P_p) and the volume fraction (ϕ_s) and length (L)

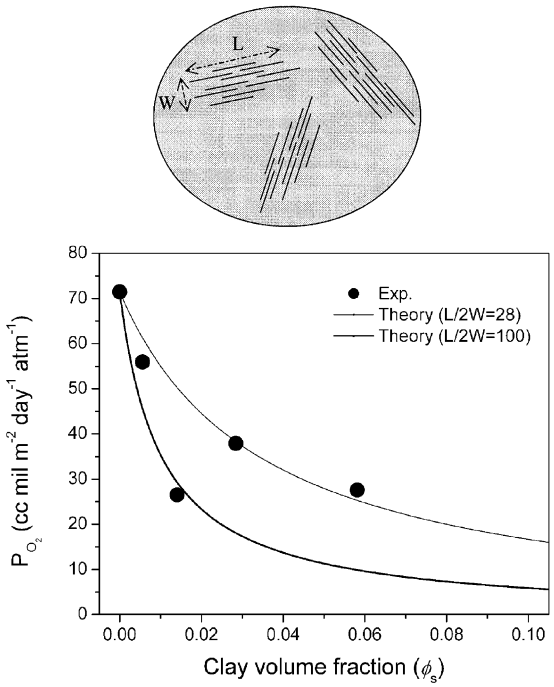

Fig. 8. Oxygen permeability of the crosslinked polyester–clay nanocomposites as a function of clay volume fraction at 40 °C and 90% relative humidity. The filled circles represent the experimental data. Theoretical fits based on the tortuosity for different aspect ratios ($L/2W$) are also shown. The illustration depicts an idealized morphology of the polyester–clay nanocomposite.

and width (W) of the sheets as [27]

$$\frac{P_s}{P_p} = \frac{1 - \phi_s}{1 + \frac{L}{2W}\phi_s}$$

The above expression assumes that the sheets are placed such that the sheet plane is perpendicular to the diffusive pathway. Recently, extensions to the tortuosity-based model to include both orientational order and state of dispersion of the sheets in addition to the concentration and sheet dimension variables were proposed [29]. There it was shown that the nanocomposites could adopt variable widths or lengths depending on the state of dispersion. The width of the basic structural unit of montmorillonite (a single aluminosilicate sheet) is well defined at $W \sim 1$ nm, however, the length displays a rather large distribution ranging between 100 nm and several microns. For the remainder of the discussion we shall implicitly assume a uniform platelet size distribution. Furthermore, the effective length and width of the nanocomposite can change rapidly through aggregation as shown in the schematic in Fig. 8. This raises the issue of whether diffusion within the aggregates itself is a possibility, but for the purposes here we shall assume that the aggregates of silicate sheets are essentially impermeable. We also ignore the possibility of trapping of the penetrant within these dense aggregates.

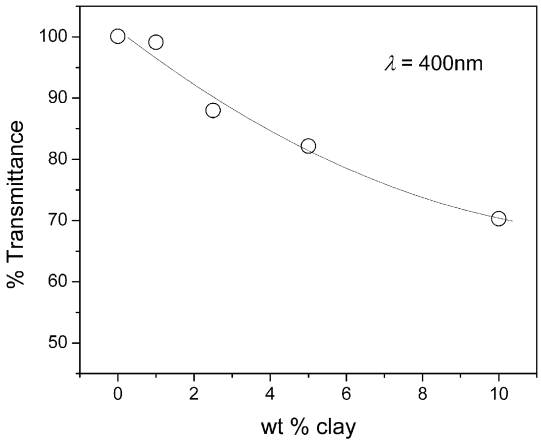

Fig. 9. Dependence of the percentage of light transmitted through the polymer nanocomposites on the clay concentration. The wavelength of light used is also shown.

The permeability of O_2 in the crosslinked polyester films is shown in Fig. 8 as a function of the volume fraction of clay. As expected, the permeability of O_2 through the crosslinked polyester nanocomposite films decreases relative to the pure crosslinked polyester film. Therefore, in terms of barrier properties, the behavior manifested is in keeping with the expectation. More importantly, we note that the decrease in O_2 permeability at 2.5 wt% clay content is greater than at other concentrations. This is in agreement with the behavior observed in the G', G'' and tensile modulus data. We note that this effect appears to be real, in that, fresh batches of resin–clay mixtures were used for each of the characterization experiments discounting the possibility of error in the preparation stage. The two curves shown in Fig. 8 represent two different values of $L/2W$ used in the above expression. The thick and thin lines represent the decrease in permeability predicted by the above expression for two effective aspect ratios, $L/2W = 100$ and 28, respectively, representing different degrees of aggregation. The 2.5 wt% data point corresponds closely to the effective $L/2W$ value of 100 indicative of greater dispersion of the silicate sheets. At higher clay concentrations, the decrease in permeability follows a different curve best fit by an $L/2W$ value of 28 implying a higher degree of aggregation. This implies that the degree of aggregation increases with the clay concentration, supported by the TEM micrographs shown in Fig. 3. At 2.5 wt% it was found that limited exfoliation on more global scale also occurred in addition to the intercalated/exfoliated aggregates. Accordingly, the decrease in permeability is also far greater. The improvement in permeability for the nanocomposite containing 2.5 wt% clay over the pure crosslinked polymer is approximately a factor of 2.7. The barrier property of nanocomposites is profoundly impacted by the morphology of polymer nanocomposites and here again the importance of delineating the morphology at different scales becomes important.

3.5. Optical properties

One of the attractive prospects of nanoscale dispersion of ~300 nm silicate platelets in a polymer matrix is the formation of nanocomposites that are optically clear [25]. The crosslinked polyester–clay nanocomposites prepared were optically clear even at 10 wt% clay content. Dependence of the thickness normalized % transmittance on clay concentration in the nanocomposites is shown in Fig. 9. The drop in transmittance ranges from being negligible at 1 wt% to 10% at 2.5 wt%, and 20% at 5 wt% clay. At 10 wt% clay concentration, there is ~30% loss in transmittance due to scattering and/or absorption. Here again, the state of dispersion and orientation of the platelets governs the optical clarity of the nanocomposite films. If complete delamination and homogeneous dispersion of the aluminosilicate sheets were achieved, it is possible that fairly high concentrations of clay may be incorporated with lower losses in the optical clarity.

4. Conclusions

Polyester–clay nanocomposites were prepared by dispersing methyl tallow bis-2-hydroxyethyl quaternary ammonium chloride modified montmorillonite in pre-promoted polyester resin and subsequently crosslinked at room temperature. The formation of a nanocomposite was confirmed by X-ray diffraction and TEM. The morphology has been studied at different length scales and is best described as a dispersion of intercalated/exfoliated aggregates of clay sheets in the matrix. Thermal, rheological, mechanical, gas transport and optical transmission properties of the crosslinked polyester–clay nanocomposites were characterized. The most important finding is that although there is firm evidence showing the formation of a nanocomposite structure, the tensile modulus, and loss and storage modulus exhibit a progressively decreasing trend with increasing clay concentration. In addition, the rate of thermal degradation is slightly but progressively hastened upon formation of a nanocomposite. These trends have been explained on the basis of a progressive decrease in the degree of crosslinking with increasing clay concentration. While this explanation is reasonable, we note that lack of detailed knowledge of the structure of the polyester resin prevents a more detailed explanation and therefore, it is more of a hypothesis than fact. Oxygen permeability in the matrices was found progressively reduced with increasing clay concentration, in keeping with the increase in the tortuous path for a diffusing penetrant. The barrier properties were found to correlate well with the observed morphology. The reduction in the loss and storage modulus, tensile modulus and oxygen permeability values at the 2.5 wt% clay concentration was found to be greater compared to that seen at higher concentrations. This behavior was traced to the exfoliation occurring at a more global scale in the 2.5 wt% case presumably leading to a greater drop in the degree of crosslinking. However, we do not discount the possibility of other sources that could account for this property reduction, such as the clay–modifier–polymer interface and the chemical effects of the organic modifier on the matrix resin. Establishing the morphological hierarchy in polymer–clay nanocomposites is demonstrated to be the key factor in developing an understanding of structure–property relationships in these systems.

Acknowledgements

The authors sincerely acknowledge the partial funding of this work by the NIST/Advanced Technology Program.

References

[1] Usuki A, Kojima Y, Kawasumi M, Okada A, Fukushima Y, Kurauchi T, Kamigaito O. J Mater Res 1993;8:1179.
[2] Kojima Y, Usuki A, Kawasumi M, Okada O, Fukushima Y, Kuruachi T, Kamaigaito O. J Mater Res 1993;8:1185.
[3] Kojima Y, Usuki A, Kawasumi M, Okada A, Kurauchi T, Kamigaito O. J Polym Sci A: Polym Chem 1993;31:983.
[4] Lan T, Pinnavaia TJ. Chem Mater 1994;6:2216.
[5] Wang Z, Pinnavaia TJ. Chem Mater 1998;10:3769.
[6] Liu L, Qi Z, Zhu X. J Appl Polym Sci 1999;71:1133.
[7] Zeng C, Lee JL. Macromolecules 2001;34:4098.
[8] Gilman JW. Appl Clay Sci 1999;15:31.
[9] Gilman JW, Jackson CL, Morgan AB, Harris R, Manias E, Giannelis EP, Wuthenow M, Hilton D, Phillips SH. Chem Mater 2000;12:1866.
[10] Vaia RA, Price G, Ruth PN, Nguyen HT, Lichtenhan J. Appl Clay Sci 1999;15:67.
[11] Kojima Y, Usuki A, Kawasumi M, Okada A, Kurauchi T, Kamigaito O. J Appl Polym Sci 1993;49:1259.
[12] Lincoln DM, Vaia RA, Sanders JH, Philips SD, Cutler JN, Cerbus CA. Polym Mater Sci Engng 2000;82:230.
[13] Yano K, Usuki A, Okada A, Kuruachi T, Kamigaito O. J Polym Sci A: Polym Chem 1993;31:2493.
[14] Yano K, Usuki A, Okada A. J Polym Sci A: Polym Chem 1997;35:2289.
[15] Lan T, Padmananda DK, Pinnavaia TJ. Chem Mater 1994;6:573.
[16] Matayabas JC, Turner SR. In: Pinnavaia TJ, Beall GW, editors. Polymer–clay nanocomposites. New York: Wiley, 2001. p. 207–26.
[17] Messersmith PB, Giannelis EP. J Polym Sci A: Polym Chem 1995;33:1047.
[18] Okamoto M, Moritaa S, Taguchi H, Kim YH, Kataka T, Tateyama H. Polymer 2000;41:3887.
[19] Tseng CR, Wu JY, Lee HY, Chang FC. Polymer 2001;42:10063.
[20] Sur GS, Sun HL, Lyu SG, Mark JE. Polymer 2001;42:9783.
[21] Vaia RA, Ishii H, Giannelis EP. Chem Mater 1993;5:1694.
[22] Kornmann X, Berglund LA, Sterte J, Giannelis EP. Polym Engng Sci 1998;38:1351.
[23] Suh DJ, Lim YT, Park OO. Polymer 2000;41:8557.
[24] Bandyopadhyay S, Giannelis EP. Polym Mater Sci Engng 2000;82:208.
[25] Strawhecker KE, Manias E. Chem Mater 2000;12:2943.
[26] Krishnamoorti R, Vaia RA, Giannelis EP. Chem Mater 1996;8:29.
[27] Nielsen LE. J Macromol Sci Chem 1967;A1:929.
[28] Beall GW. In: Pinnavaia TJ, Beall GW, editors. Polymer–clay nanocomposites. New York: Wiley, 2001. p. 267–79.
[29] Bharadwaj RK. Macromolecules 2001;34:9189.